

# Survival of $\Phi_0/2$ periodicity in presence of incoherence in asymmetric Aharonov-Bohm rings

Colin Benjamin,<sup>1,\*</sup> Swarnali Bandopadhyay,<sup>2,†</sup> and A. M. Jayannavar<sup>1,‡</sup>

<sup>1</sup>*Institute of Physics, Sachivalaya Marg, Bhubaneswar 751 005, Orissa, India*

<sup>2</sup>*S N Bose National Center for Basic Sciences, JD Block,  
Sector III, Salt Lake City, Kolkata 700098, India*

(Dated: February 1, 2008)

Magneto conductance oscillations periodic in flux with periodicity  $\Phi_0$  and  $\Phi_0/2$  are seen in asymmetric Aharonov-Bohm rings as a function of density of electrons or Fermi wave vector. Dephasing of these oscillations is incorporated using a simple approach of wave attenuation. In this work we study how the excitation of the  $\Phi_0/2$  oscillations and the accompanying phase change of  $\pi$  are affected by dephasing. Our results show that the  $\Phi_0/2$  oscillations survive incoherence, i.e., dephasing, albeit with reduced visibility while incoherence is also unable to obliterate the phase change of  $\pi$ .

PACS numbers: 72.10.-d, 73.23.-b, 05.60.Gg, 85.35.Ds

Keywords: D. Electron Transport, A. Nanostructures, D. Aharonov-Bohm oscillations, D. Dephasing

The  $\Phi_0/2$  periodicity was a puzzle in mesoscopic physics in its early days. Among the first experiments<sup>1</sup> which were purported to measure the magneto resistance oscillations in normal metal cylinders, observed a  $\Phi_0/2$  periodicity. However, theoretical calculations<sup>2,3,4</sup> on strictly one-dimensional normal metal ballistic rings argued that only  $\Phi_0$  periodicity should be observed. The experiment which observed these  $\Phi_0/2$  oscillations were backed by theoretical work which predicted these based on weak localization<sup>5,6</sup>. In the recent works of Pedersen, et.al.,<sup>7</sup> and Hansen, et.al.,<sup>8</sup>, the AB effect in a one dimensional *GaAs/Ga<sub>0.7</sub>Al<sub>0.3</sub>As* ring at low magnetic fields has been investigated. In their work they observe the fundamental  $\Phi_0$  periodicity in the magneto-conductance as expected. Moreover, as the density (in effect the Fermi energy) is varied they observe phase shifts of  $\pi$  in the magneto conductance oscillations and  $\Phi_0/2$  periodicity at particular values of the Fermi energy. They have found good agreement of their results with the completely phase coherent transport theory<sup>9</sup> of electrons in an asymmetric Aharonov-Bohm ring in the single channel regime. Asymmetry of the AB ring was crucial in understanding these observations. Such behavior has also been observed in an earlier experiment<sup>10</sup>, and has generated a lot of interest in relation to the problem of phase measurement.

The endeavor of this work is not on the origin of the  $\Phi_0/2$  periodicity but on the effect of inelastic or phase breaking scattering on these. Our results indicate that the phase shift of  $\pi$  in AB oscillations and halving of the fundamental  $h/e$  periodicity survives in-spite of dephasing albeit with reduced visibility in AB oscillations. There are many ways to phenomenologically model inelastic scattering in mesoscopic devices. Among the first was by Büttiker<sup>11</sup> who considered an electron reservoir coupled by a lead to a mesoscopic system as a phase breaker or inelastic scatterer (voltage probe). This approach has been widely used to investigate the effect of dephasing on the conductance. This method which uses voltage probes as dephaser's is interesting because of it's conceptual clarity and it's close relation to experiments.

It provides a useful trick to simulate lack of full coherence in transport properties. This method of addressing the problem of dephasing has the advantage that inelastic phase randomizing processes can be incorporated by solving an elastic time independent scattering problem. Beyond Büttiker's model, optical potential,<sup>12,13</sup> and wave attenuation (stochastic absorption) models<sup>14,15</sup> have also been used to simulate dephasing. However in the afore-said models energy relaxation and thermal effects<sup>16</sup> are ignored. Thermal effects can be incorporated by taking into account thermal distribution (Fermi-Dirac function) of electrons. In mesoscopic systems, transmission functions are more often than not constant over the energy range wherein transport occurs (at low temperatures) and one can ignore energy relaxation or "vertical flow"<sup>17</sup> of electron carrier's in these systems. Brouwer and Beenakker have corrected some of the problems associated with voltage probe and optical potential models, (see Refs.[14,18] for details), and given a general formalism for calculating the conductance(G) in the presence of inelastic scattering. Furthermore, methods based on optical potentials and wave attenuation can make use of this above formalism. In this work we use the method of wave attenuation.

This method of wave attenuation has been used earlier to study dephasing of AB oscillations<sup>14</sup> and calculating sojourn times in quantum mechanics<sup>19</sup>. The wave attenuation model has been shown to be better than the optical potential model (which has in built spurious scattering)<sup>14</sup>. We use the well known S-Matrix method to calculate the conductance and therein we see the  $\Phi_0/2$  periodicity as also the phase change of  $\pi$  across such an excitation of the  $h/2e$  oscillations. The system we consider, is shown in FIG. 1, is an asymmetric Aharonov-Bohm loop with upper and lower arm lengths  $l_1$  and  $l_2$  and circumference  $L = l_1 + l_2$ , coupled to two leads which in turn are connected to two reservoirs at chemical potentials  $\mu_1$  and  $\mu_2$ . Inelastic scattering is assumed to be absent in the leads while it is present in the reservoirs, and in the loop we introduce incoherence via wave attenua-

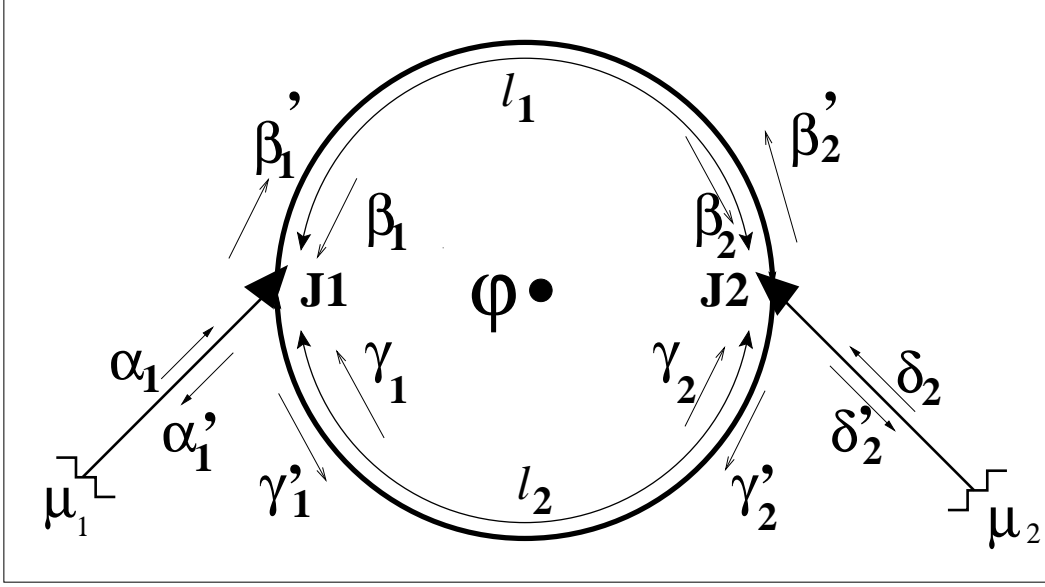


FIG. 1: Aharonov - Bohm ring geometry.

tion to simulate inelastic scattering. The S matrix for the left coupler yields the amplitudes  $O_1 = (\alpha'_1, \beta'_1, \gamma'_1)$  emanating from the coupler in terms of the incident waves  $I_1 = (\alpha_1, \beta_1, \gamma_1)$ , and for the right coupler yields the amplitudes  $O_2 = (\delta'_2, \beta'_2, \gamma'_2)$  emanating from the coupler in terms of the incident waves  $I_2 = (\delta_2, \beta_2, \gamma_2)$ . The S-matrix for either of the couplers<sup>3</sup> is given by-

$$S = \begin{pmatrix} -(a+b) & \sqrt{\epsilon} & \sqrt{\epsilon} \\ \sqrt{\epsilon} & a & b \\ \sqrt{\epsilon} & b & a \end{pmatrix}$$

with  $a = \frac{1}{2}(\sqrt{1-2\epsilon} - 1)$  and  $b = \frac{1}{2}(\sqrt{1-2\epsilon} + 1)$ . Herein,  $\epsilon$  plays the role of a coupling parameter. The maximum coupling between reservoir and loop is  $\epsilon = \frac{1}{2}$ , and for  $\epsilon = 0$ , the coupler completely disconnects the loop from the reservoir. Inelastic scattering in the arms of the AB interferometer is taken into account by introducing an attenuation constant per unit length in the two arms of the ring, i.e., the factors  $e^{-\alpha l_1}$  (or  $e^{-\alpha l_2}$ ) in the free propagator amplitudes, every time the electron<sup>14,17</sup> traverses the upper (or lower) arms of the loop (see Fig. 1).

The waves incident into the branches of the loop are related by the S Matrices<sup>20</sup> for upper branch by-

$$\begin{pmatrix} \beta_1 \\ \beta_2 \end{pmatrix} = \begin{pmatrix} 0 & e^{ikl_1} e^{-\alpha l_1} e^{-\frac{i\theta l_1}{L}} \\ e^{ikl_1} e^{-\alpha l_1} e^{\frac{i\theta l_1}{L}} & 0 \end{pmatrix} \begin{pmatrix} \beta'_1 \\ \beta'_2 \end{pmatrix}$$

and for lower branch-

$$\begin{pmatrix} \gamma_1 \\ \gamma_2 \end{pmatrix} = \begin{pmatrix} 0 & e^{ikl_2} e^{-\alpha l_2} e^{\frac{i\theta l_2}{L}} \\ e^{ikl_2} e^{-\alpha l_2} e^{-\frac{i\theta l_2}{L}} & 0 \end{pmatrix} \begin{pmatrix} \gamma'_1 \\ \gamma'_2 \end{pmatrix}$$

These S matrices of course are not unitary  $S(\alpha)S(\alpha)^\dagger \neq 1$  but they obey the duality relation

$S(\alpha)S(-\alpha)^\dagger = 1$ . Here  $kl_1$  and  $kl_2$  are the phase increments of the wave function in absence of flux.  $\frac{\theta l_1}{L}$  and  $\frac{\theta l_2}{L}$  are the phase shifts due to flux in the upper and lower branches. Clearly,  $\frac{\theta l_1}{L} + \frac{\theta l_2}{L} = \frac{2\pi\Phi}{\Phi_0}$ , where  $\Phi$  is the flux piercing the loop and  $\Phi_0$  is the flux quantum  $\frac{hc}{e}$ . The transmission and reflection coefficients are given as follows-  $T_{21} = |\frac{\delta'_2}{\alpha_1}|^2$ ,  $R_{11} = |\frac{\alpha'_1}{\alpha_1}|^2$ ,  $R_{22} = |\frac{\delta'_2}{\delta_2}|^2$ ,  $T_{12} = |\frac{\alpha'_1}{\delta_2}|^2$  wherein wave amplitudes  $\delta'_2, \delta_2, \alpha'_1, \alpha_1$  are as depicted in FIG. 1.

The transmission coefficient  $T_{21}$  from reservoir 1 to 2 is not symmetric under flux reversal which is in contradiction with Onsager's symmetry condition, and is due to the fact that current conservation as also unitarity have been violated (due to wave attenuation). As, is well known there can be real absorption of photons but there cannot be any real absorption of electrons. The absorption is interpreted as electron scattering into different energy channels and the way these electrons are re-injected back into the system becomes important<sup>21,22</sup>. Following the earlier treatments (see the details in Refs. [14,18]), the conductance in dimensionless form after proper re-injection of carriers is given by -

$$G = T_{21} + \frac{(1 - R_{11} - T_{21})(1 - R_{22} - T_{21})}{1 - R_{11} - T_{21} + 1 - R_{22} - T_{12}}. \quad (1)$$

The first term in Eq. 1, i.e.,  $T_{21}$  represents the phase coherent contribution, while the second term accounts for electrons that are re-injected after inelastic scattering. This represents the phase incoherent contribution to the conductance.  $G$  respects Onsager's symmetry  $G(\Phi) = G(-\Phi)$ , and thus the phase of AB oscillations can only change<sup>10</sup> by  $\pm\pi$ .

As previously mentioned our interest in this work is to

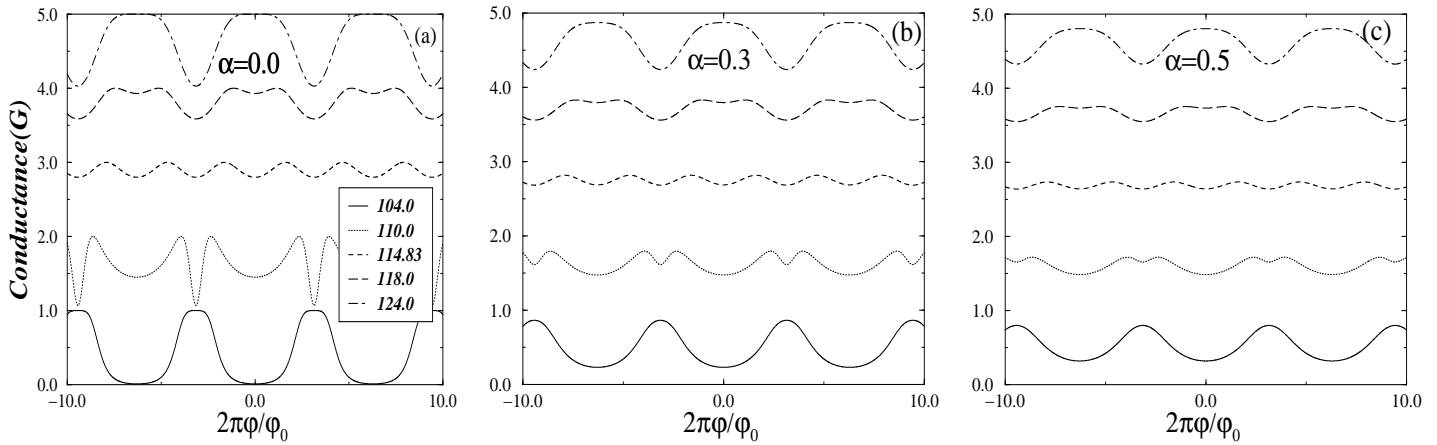


FIG. 2: Conductance ( $G$ ) for lengths  $l_1/L = 0.425$ ,  $l_2/L = 0.575$  and coupling parameter  $\epsilon = 0.5$  (strong coupling) for different values of the Fermi wave-vector  $k_f L$ . The legend in FIG. 2(a) remains same for 2(b) and 2(c).

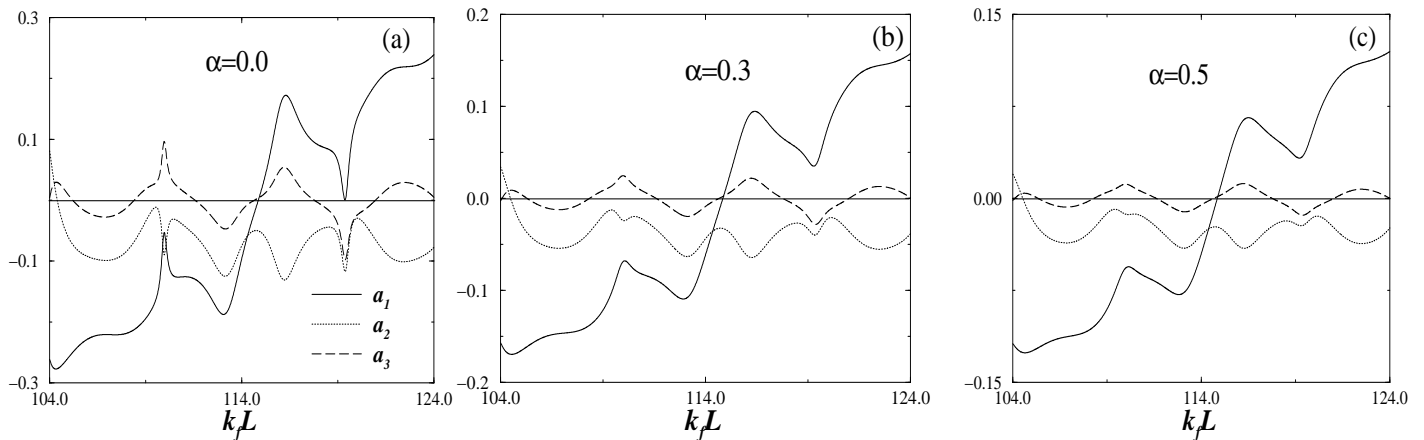


FIG. 3: Harmonics for lengths  $l_1/L = 0.425$ ,  $l_2/L = 0.575$  and coupling parameter  $\epsilon = 0.5$  (strong coupling) as a function of the dimensionless Fermi wave-vector  $k_f L$ . The legend in FIG. 3(a) remains same for 3(b) and 3(c).

observe the effect of incoherence on the  $\Phi_0/2$  oscillations in single channel ballistic rings. We choose an asymmetric AB ring with degree of asymmetry denoted by the difference in arm lengths  $\Delta = l_1 - l_2 = 0.15$ , and circumference  $L = 1.0$  in accordance with the experimental realization as in Ref. [7]. The change in Fermi energy of injected electrons implies varying the density of electrons in the system. So, when we scan the whole range of the dimensionless wave vector  $k_f L$  from 0.0 to 200.0 we come across  $\Phi_0/2$  periodicities at particular values of the Fermi wave vector  $k_f L$ , notably at 10.83, 114.8302 and 136.5. We now restrict ourselves to the particular range (Fermi energy) and parameters (length's and coupling) corresponding to the experimental situation studied earlier as in Refs. [7,8]. In our treatment  $\alpha$  represents the incoherence parameter (degree of dephasing). The plot of the dimensionless conductance  $G$  as a function of flux in the range  $104.0 \leq k_f L \leq 124.0$ , with de-

gree of incoherence  $\alpha = 0$  is shown in FIG. 2(a). Similarly in FIG. 2(b) and 2(c) we plot  $G$  for  $\alpha = 0.3$  and  $\alpha = 0.5$ , for the same system parameters and range of  $k_f L$ . The plots for  $k_f L > 104.0$  are each shifted by a factor of 1 for clarity. The  $\Phi_0/2$  periodicities are clearly marked at  $k_f L = 114.8302$ , and also across this range of  $k_f L$  and excitation of the  $h/2e$  harmonic, phase changes by  $\pi$ . Thus phase shift of  $\pi$  along with halving of the fundamental  $h/e$  period is clearly seen as a function of Fermi-wavevector (density) consistent with the experimental observations. Importantly, this observed behavior survives dephasing with reduced visibility, therefore the observed results need not be attributed to complete phase coherence in the system. One conclusion which can be drawn from the afore drawn figures is that incoherence reduces the visibility of AB oscillations as expected. However, this dephasing is unable to shift the position of the  $\Phi_0/2$  oscillations noticeably, for the chosen coupling

parameter.

The reason why we observe  $\Phi_0/2$  periodic oscillations at these particular values of  $k_f L$  is because at these values both  $h/e$  as well as  $h/3e$  harmonics are extremely weak as also the higher harmonics and therefore exclusive  $\Phi_0/2$  oscillations are seen. The  $k_f L$  values wherein exclusive  $\Phi_0/2$  oscillations are seen are at  $k_f L = 10.8335, 114.8302$  and  $136.5$ , in the range  $0.0 < k_f L < 200.0$  for the same physical parameters. In FIG.3(a),(b) and (c), we plot the harmonics as a function of the dimensionless Fermi wave-vector  $k_f L$  for  $\alpha = 0.0, 0.3$  and  $0.5$ . The harmonics are calculated as follows-

$$a_n = \frac{1}{\pi} \int_0^{2\pi} G \cos(n\theta) d\theta \quad (2)$$

At the ' $k_f L$ ' value, wherein  $\Phi_0/2$  oscillations dominate, the first and third harmonic's do not contribute at all to the conductance as can be seen from the FIG's.3(a)-(c). We observe that increasing dephasing ( $\alpha$ ) does not noticeably shift the ' $k_f L$ ' value, wherein  $\Phi_0/2$  oscillations dominate. We also see that the higher harmonic  $a_3 = h/3e$  goes faster to zero and therefore these contributions are washed out and  $\Phi_0/2$  oscillations survive dephasing albeit with reduced strengths. The fact that the Fermi-wavevector  $k_f L$  (at which  $\Phi_0/2$  oscillations occur) does not noticeably shift is peculiar to the coupling parameter chosen, which for the above cases is  $0.5$  (maximal coupling). However, for some other physical param-

eters there may be a small shift in Fermi-wavevector  $k_f L$  with increasing incoherence. For example, for the case  $\epsilon = 0.44$  (waveguide coupling) the  $\Phi_0/2$  oscillations are observed at  $k_f L = 52.0$  at  $\alpha = 0.0$ , for the same length parameters as in FIG. 2, but when this incoherence parameter is increased we see these oscillations are shifted to different values of  $k_f L$ , e.g., for  $\alpha = 0.5$  these are seen at  $k_f L = 51.95$ . For this coupling too we indeed observe phase change of  $\pi$  in AB oscillations along with period halving, consistent with our previous observations. Shifts in Fermi-wavevector are small for maximal coupling but when coupling strength is decreased these shifts become more noticeable.

In conclusion, we have observed  $\Phi_0/2$  oscillations as we vary the density of electrons which is similar to varying the Fermi wave vector consistent with experimental observations. The  $\Phi_0/2$  oscillations are shifted by dephasing (noticeably small for maximal coupling), apart from the reduction of their strengths. The phase change of  $\pi$  which occurs across the excitation of  $h/2e$  oscillations is seen to be independent of dephasing. Thus complete phase coherence of electron over the entire sample is not necessary to observe these effects.

### Acknowledgments

One of us SB thanks the Institute of Physics, Bhubaneswar for hospitality.

- 
- \* Electronic address: colin@iopb.res.in  
 † Electronic address: swarnali@bose.res.in  
 ‡ Electronic address: jayan@iopb.res.in  
<sup>1</sup> D. Yu. Sharvin and Yu. V. Sharvin, JETP Lett. **34**, 272 (1981).  
<sup>2</sup> M. Büttiker, Y. Imry, R. Landauer, Phys. Lett. **96A**, 365 (1983).  
<sup>3</sup> M. Büttiker, Y. Imry and M. Ya. Azbel, Phys. Rev. A **30**, 1982 (1984).  
<sup>4</sup> Y. Gefen, Y. Imry and M. Ya. Azbel, Phys. Rev. Lett. **52**, 129 (1984).  
<sup>5</sup> B. L. Altshuler, A. G. Aronov and B. Z. Spivak, JETP Lett. **33**, 94 (1981).  
<sup>6</sup> S. Washburn and R. A. Webb, Adv. Phys. **35**, 375(1986); S. Washburn and R. A. Webb, Rep. Prog. Phys. **55**, 1311 (1992).  
<sup>7</sup> S. Pedersen, A. E. Hansen, A. Kristensen, C. B. Sorensen, and P. E. Lindelof, Phys. Rev. B **61**, 5457 (2000).  
<sup>8</sup> A. E. Hansen, S. Pedersen, A. Kristensen, C. B. Sorensen, and P. E. Lindelof, cond-mat/9909246.  
<sup>9</sup> M. Büttiker, *SQUID'85- Superconducting Quantum Interference Devices and their Applications*, ed. H. D. Hahlbohm and H. Lübbig (Walter de Gruyter, Berlin), p. 529 (1985).  
<sup>10</sup> A. Yacoby, M. Heiblum, D. Mahalu and H. Shtrikman, Phys. Rev. Lett. **74**, 4047 (1995).

- <sup>11</sup> M. Büttiker, Phys. Rev. B **33**, 3020 (1986); IBM J. Res. Dev. **32**, 63 (1988).  
<sup>12</sup> D. K. Ferry and J. R. Barker, Appl. Phys. Lett. **74**, 582 (1999).  
<sup>13</sup> A. M. Jayannavar, Phys. Rev. B **49**, 14718 (1994); A. K. Gupta and A. M. Jayannavar, Phys. Rev. B **52**, 4156 (1995).  
<sup>14</sup> Colin Benjamin and A. M. Jayannavar, Phys. Rev. B **65**, 153309 (2002).  
<sup>15</sup> Sandeep K. Joshi, D. Sahoo and A. M. Jayannavar, Phys. Rev. B **62**, 880 (2000);  
<sup>16</sup> N. A. Mortensen, A. P. Jauho and K. Flensberg, Superlattices and Microstructures **28**, 67 (2000).  
<sup>17</sup> S. Datta, *Electron Transport in mesoscopic systems* (Cambridge University press, Cambridge, 1995).  
<sup>18</sup> P. W. Brouwer and C. W. J. Beenakker, Phys. Rev. B **55**, 4695 (1997); P. W. Brouwer, Ph.D. thesis, Instituut-Lorentz, University of Leiden, The Netherlands, 1997.  
<sup>19</sup> Colin Benjamin and A. M. Jayannavar, Solid State Commun. **121**, 591 (2002).  
<sup>20</sup> M. Cahay, H. Grubin and S. Bandopadhyay, Phys. Rev. B **39**, 12989 (1989).  
<sup>21</sup> M. Büttiker, Pramana J. Phys. **58**, 241 (2002).  
<sup>22</sup> T. P. Pareek, S. K. Joshi and A. M. Jayannavar, Phys. Rev. B **57**, 8809 (1998).